Biophysical Journal, Volume 96

Supplementary Material

Thermal Stability of Apolipoprotein A-I in High Density Lipoproteins by Molecular Dynamics

Martin K. Jones, Andrea Catte, James C. Patterson, Feifei Gu, Jianguo Chen, Ling Li, and Jere P. Segrest

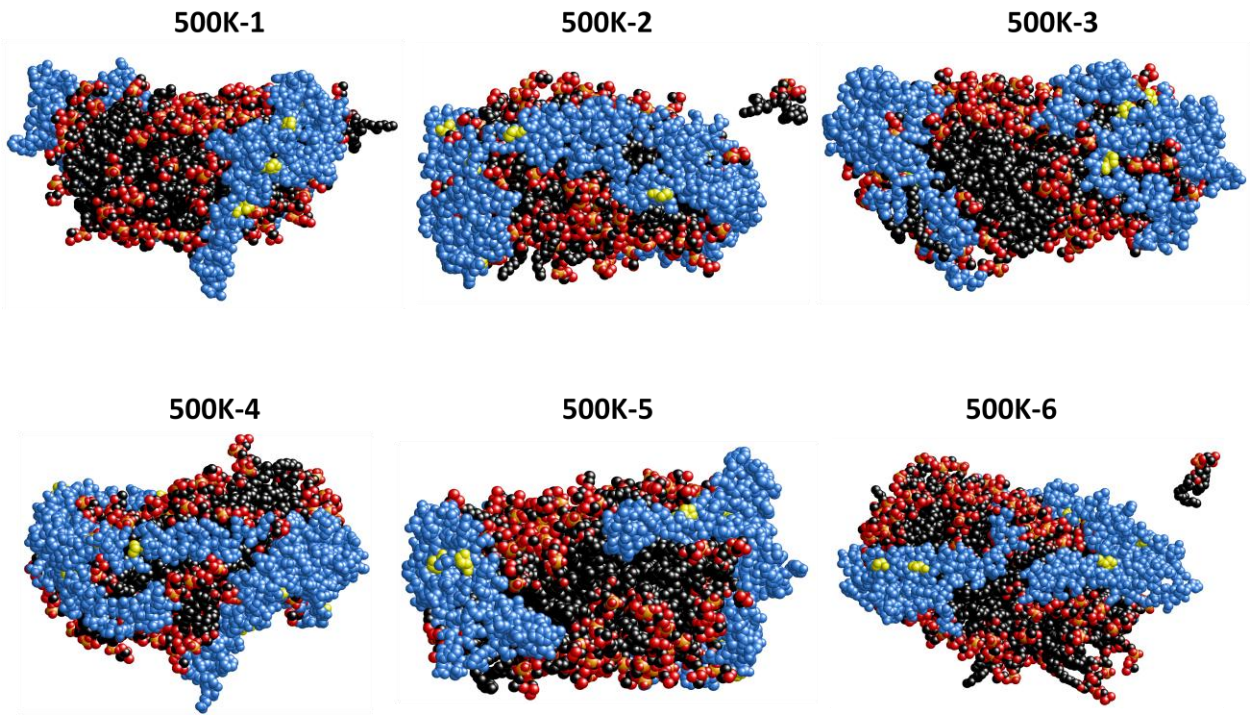

Figure S1. Structures of each of the six 500 K simulations of 100:2 at 20 ns. (***500K-1-3)*** Three simulations of independent particle I-1. (***500K-4-6)*** Three simulations of independent particle I-2. The structures in spacefilling representation are viewed from the terminal domain side of the particles with the same orientations as in **Fig. 2**. *(Skyblue)* protein; *(yellow)* prolines; *(black)* POPC acyl chains*; (red and gold)* headgroups.

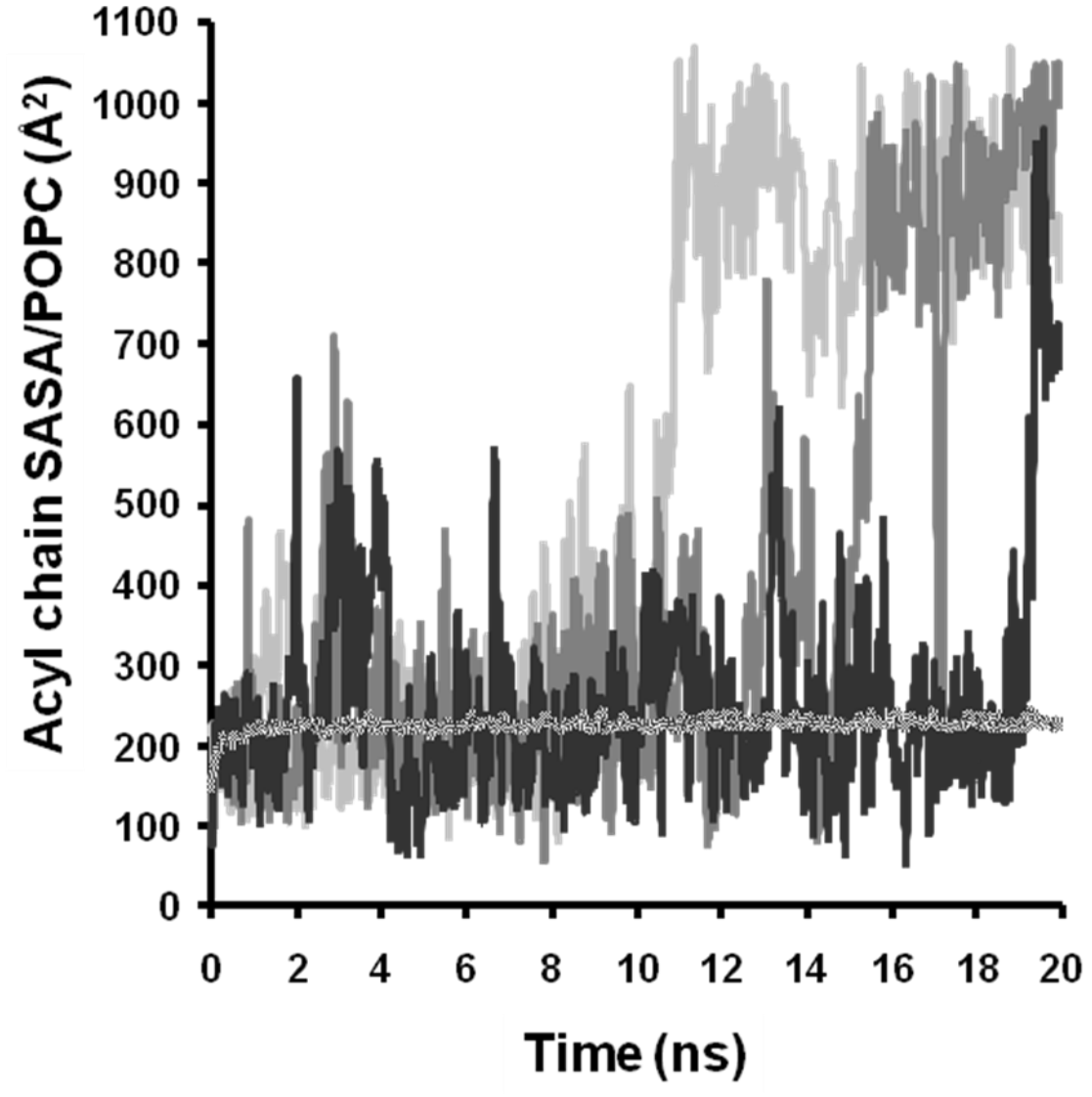

Figure S2. Changes in SASA of the acyl chains per POPC for each of the three single POPC molecules desorbed from its 100:2 particle at 500 K plotted over 20 ns compared with changes in mean SASA of the six simulations at each time point. *(Widely fluctuating lines)* changes in SASA of each of the three single POPC molecules desorbed from its 100:2 particle at each time point; *(narrowly fluctuating line)* changes in mean SASA of the six simulations at each time point.

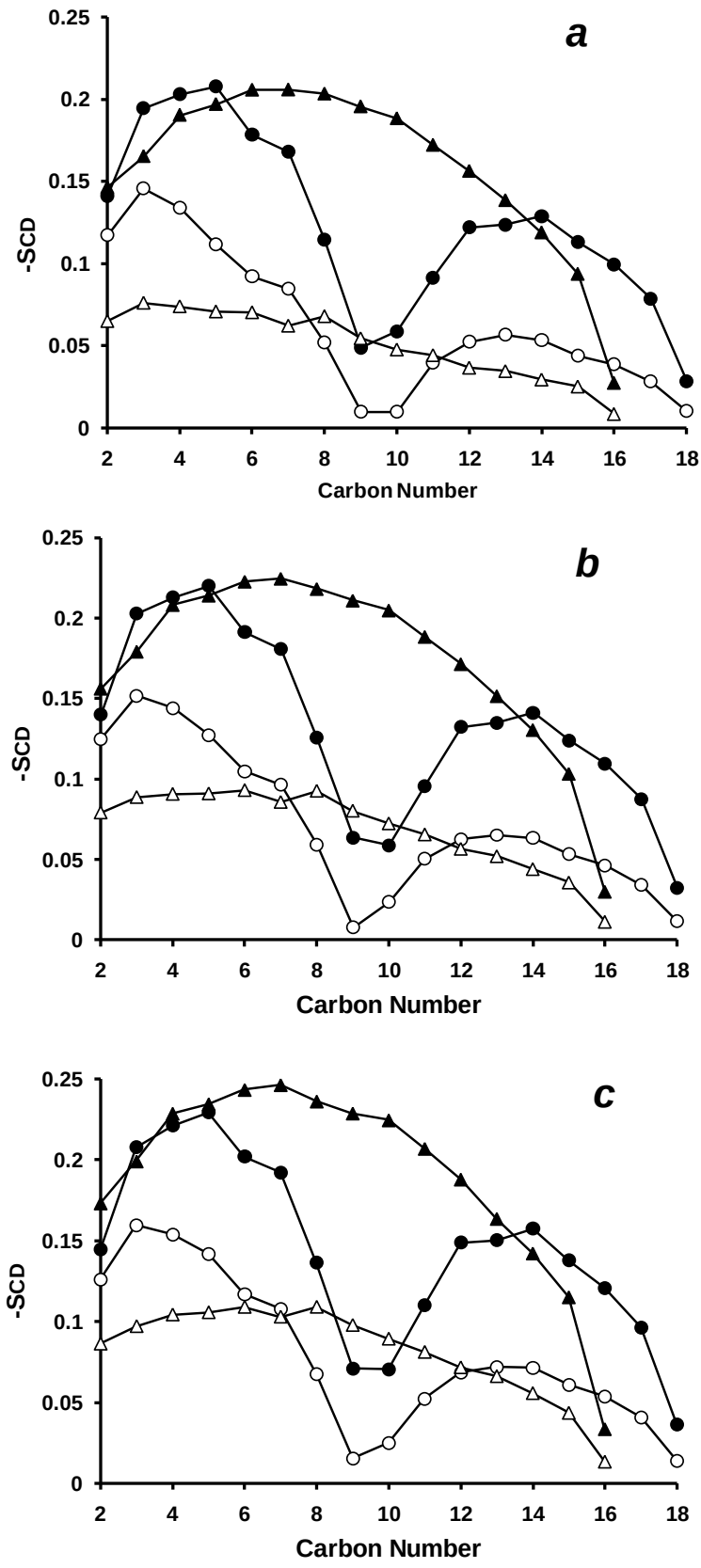

Figure S3. Average order parameters calculated for POPC within and not within 6, 8 and 10 Å over the last 40% of simulations at 310 K for I-1 and I-2 particles.

The values for the SCD are averages over both hydrogen atoms on each methylene carbon and are shown as triangles for the sn-1 (palmitoyl) chain and as circles for the sn-2 (oleoyl) chain. ***(a)*** Plot of average order parameters calculated for all POPC within *(open symbols)* and not within *(closed symbols)* 6 Å of protein. ***(b)*** Plot of average order parameters calculated for all POPC within *(open symbols)* and not within *(closed symbols)* 8 Å of protein. ***(c)*** Plot of average order parameters calculated for all POPC within *(open symbols)* and not within *(closed symbols)* 10 Å of protein.

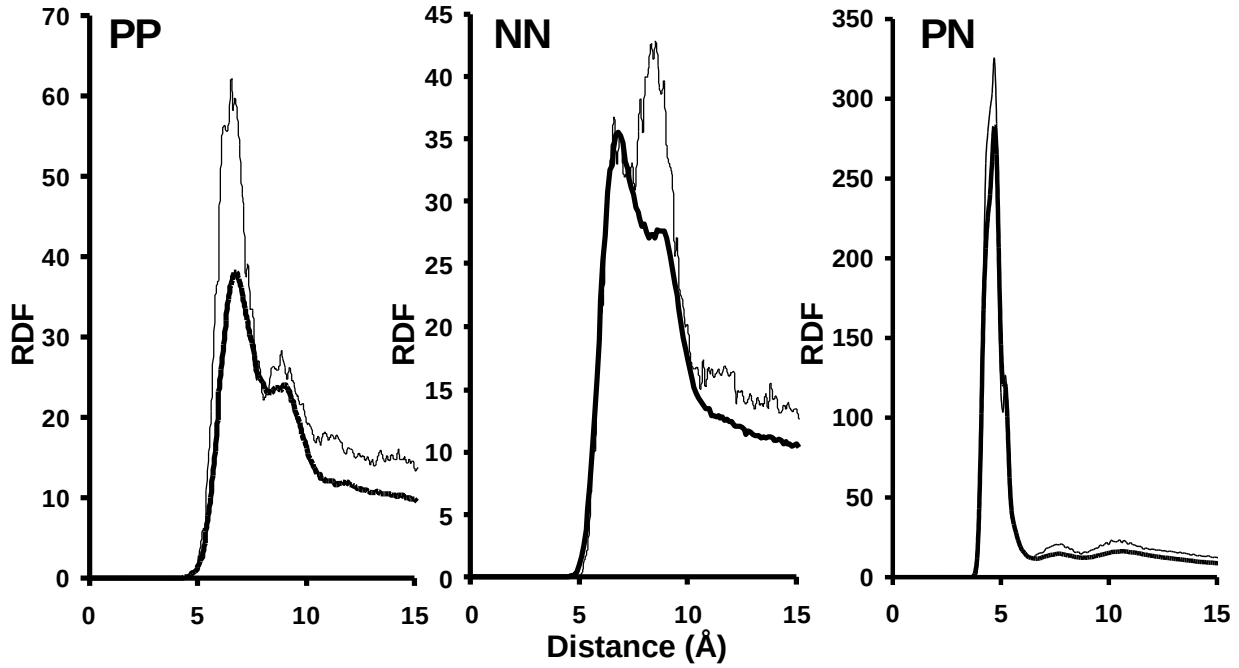

Figure S4. Mean radial distribution functions (RDF) of: phosphorus (PP), nitogen (NN) and phosphorous-nitrogen (PN) for the POPC for the six 100:2 particle MD simulations plotted over the last 20% of the 20 ns simulations. *(Gray lines)* 310 K simulations; *(black lines)* 500 K simulations.

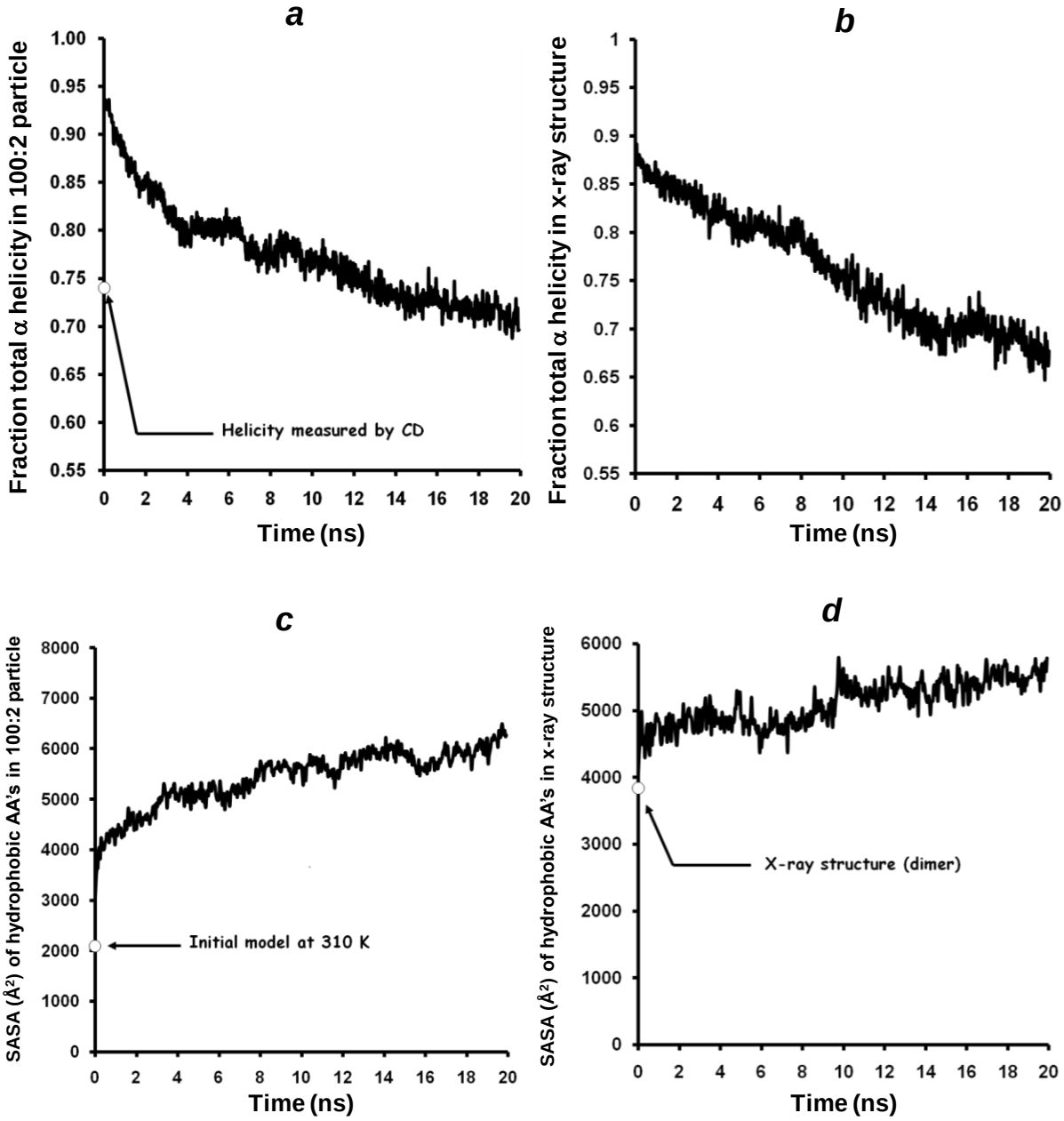

Figure S5. Changes in global α helicity and solvent accessible surface area of hydrophobic amino acid residues during 20 ns MD simulations at 500 K of the 100:2 particles I-1 and I-2 versus the control Δ43apoA-I. ***(a)*** Changes in global α helicity of the six 100:2 particle MD simulations at 500 K plotted over 20 ns. *(Gray lines)* changes in global α helicity of each of the six individual simulations at each time point; *(black line)* change in mean global α helicity of the six simulations at each time point. ***(b)*** Changes in global α helicity of the close AB and CD pairs of each of the two MD simulations performed on the control Δ40apoA-I structure at 500 K plotted over 20 ns. *(Gray lines)* changes in global α helicity for each of the four close pairs at each time point; *(black line)* change in mean global α helicity of the four close pair simulations at each time point. ***(c)*** Changes in solvent accessible surface areas (SASA) of the hydrophobic amino acid residues for the six 100:2 particle MD simulations at 500 K

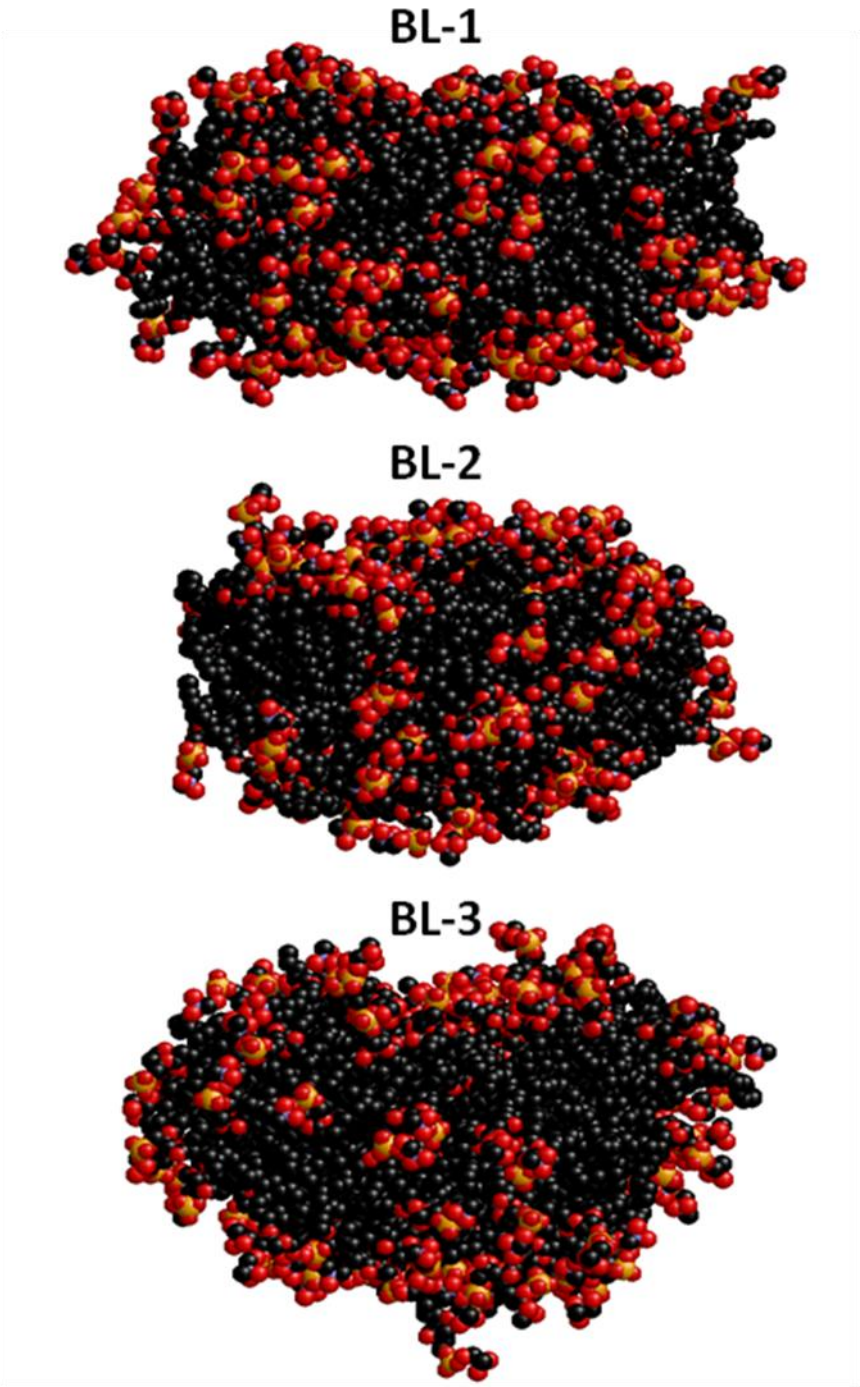

Figure S6. Structures of the three 500 K simulations of 'naked" lipid bilayer discs containing 100 POPC at 20 ns. The structures are in spacefilling representation. *(Black)* POPC acyl chains*; (red and gold)* headgroups.